


# Propagation of terahertz waves in nonuniform plasma slab under “electromagnetic window”

Hao Li(李郝), Zheng-Ping Zhang(张正平), and Xin Yang (杨鑫)
**Citation:**Chin. Phys. B, 2022, 31 (**3**): 035202. DOI: 10.1088/1674-1056/ac1b90
Journal homepage: http://cpb.iphy.ac.cn; http://iopscience.iop.org/cpb

**What follows is a list of articles you may be interested in**

---

## Electron acceleration during magnetic islands coalescence and division process in a guide field reconnection

Shengxing Han(韩圣星), Huanyu Wang(王焕宇), and Xinliang Gao(高新亮)
Chin. Phys. B, 2022, 31 (**2**): 025202. DOI: 10.1088/1674-1056/ac21c0

## Time-resolved radial uniformity of pulse-modulated inductively coupled $O_2$/Ar plasmas

Wei Liu(刘巍), Chan Xue(薛婵), Fei Gao(高飞), Yong-Xin Liu(刘永新), You-Nian Wang(王友年), and Yong-Tao Zhao(赵永涛)
Chin. Phys. B, 2021, 30 (**6**): 065202. DOI: 10.1088/1674-1056/abe3f5

## Numerical simulation and experimental validation of multiphysics field coupling mechanisms for a high power ICP wind tunnel

Ming-Hao Yu(喻明浩), Zhe Wang(王哲), Ze-Yang Qiu(邱泽洋), Bo Lv(吕博), and Bo-Rui Zheng(郑博睿)
Chin. Phys. B, 2021, 30 (**6**): 065201. DOI: 10.1088/1674-1056/abeb0e

## Spatio-temporal measurements of overshoot phenomenon in pulsed inductively coupled discharge

Xiang-Yun Lv(吕翔云), Fei Gao(高飞), Quan-Zhi Zhang(张权治), and You-Nian Wang(王友年)
Chin. Phys. B, 2021, 30 (**4**): 045202. DOI: 10.1088/1674-1056/abd16b

## New terahertz dispersive device for single-shot spectral measurements of terahertz pulse

Wu Yin-Zhong, Zhao Zong-Qing, Gu Yu-Qiu, Wei Lai, Cao Lei-Feng
Chin. Phys. B, 2014, 23 (**12**): 125202. DOI: 10.1088/1674-1056/23/12/125202

---

# Propagation of terahertz waves in nonuniform plasma slab under "electromagnetic window"

Hao Li(李郝)[1], Zheng-Ping Zhang(张正平)[1,2,3], and Xin Yang (杨鑫)[1,2,3,†]

[1] *College of Big Data and Information Engineering, Guizhou University, Guiyang* 550025, *China*
[2] *Semiconductor Power Device Reliability Engineering Research Center of Ministry of Education, Guizhou University, Guiyang* 550025, *China*
[3] *Key Laboratory of Micro-Nano-Electronics and Software Technology of Guizhou Province, Guiyang* 550025, *China*

(Received 24 June 2021; revised manuscript received 31 July 2021; accepted manuscript online 7 August 2021)

The application of magnetic fields, electric fields, and the increase of the electromagnetic wave frequency are up-and-coming solutions for the blackout problem. Therefore, this study considers the influence of the external magnetic field on the electron flow and the effect of the external electric field on the electron density distribution, and uses the scattering matrix method (SMM) to perform theoretical calculations and analyze the transmission behavior of terahertz waves under different electron densities, magnetic field distributions, and collision frequencies. The results show that the external magnetic field can improve the transmission of terahertz waves at the low-frequency end. Magnetizing the plasma from the direction perpendicular to the incident path can optimize the right-hand polarized wave transmission. The external electric field can increase the transmittance to some extent, and the increase of the collision frequency can suppress the right-hand polarized wave cyclotron resonance caused by the external magnetic field. By adjusting these parameters, it is expected to alleviate the blackout phenomenon to a certain extent.

**Keywords:** terahertz wave, scattering matrix method (SMM), nonuniform magnetized plasma, electric field

**PACS:** 52.40.Db, 52.25.Fi, 41.20.Jb **DOI:** 10.1088/1674-1056/ac1b90

## 1. Introduction

At velocities near or above Mach 10, atmospheric gas flowing by the hypersonic vehicle will be heated by the supersonic shock in front of the vehicle. It creates friction violently when the atmospheric gas flows around the aircraft, causing the dissociation of molecules and atoms to form an ionized flow, or so-called "plasma sheath".[1,2] The electron density of the plasma sheath can reach more than $10^{19}$ $m^{-3}$,[3] so that the electromagnetic wave energy emitted or received by the antenna window is absorbed in large amounts, making communication impossible. That is, the blackout phenomenon occurs. Many technologies have been proposed to alleviate the blackout problem,[4–9] such as aerodynamic shape, material injection, magnetic and electric field restraint, high-frequency transmission. With the development of electromagnetic materials and terahertz wave technology, additional electromagnetic fields and terahertz wave transmission have great potential in alleviating the blackout problem. The frequency of the THz wave is higher than the cut-off frequency of the high-density plasma sheath currently studied. Hence, it has excellent penetration into the sheath. The THz wave also has good anti-interference, so researchers have begun to pay attention to the transmission of terahertz waves in plasma and the influence of magnetic fields on transmission. Zhou *et al.* studied the influence of non-uniform magnetic fields on the transmission of electromagnetic waves below Ka in the sheath.[10] Zhang *et al.* studied the transmission characteristics of terahertz waves in parallel magnetized sheaths,[11] Lemmer *et al.* investigated the effects of cross electric and magnetic fields on plasma sheaths.[12] Kim *et al.* studied the sheath electron density changes near the electrode under an electric field.[13] Therefore, the transmission characteristics of terahertz waves in the plasma sheath under the action of electric and magnetic fields are worth studying. Computer numerical analysis is more comfortable and efficient than the flight test with the high cost and harsh detection conditions. It is widely used to analyze electromagnetic wave transmission characteristics in plasma, such as through using the Wentzel–Kramer–Brillouin (WKB) method, scattering matrix method (SMM), finite-difference time-domain (FDTD) method.[14–25] Yu *et al.* used the WKB method to study the transmission characteristics of terahertz waves in magnetized plasmas with different electron density distributions.[26] Numerical simulation results demonstrated that the plasma density, plasma slab thickness, plasma density models, and collision frequency significantly influence the attenuation and transmittance of terahertz waves. Guo *et al.* used the SMM to study the transmission characteristics of terahertz waves in three parabolic magnetized plasmas.[27] Numerical calculation results show that the characteristics of the absorption spectra are affected by the parameters in the first layer of plasma and the gradient of the parameters across the entire plasma. Zhang *et al.* used the FDTD to study the three types of plasma absorptions, including plasma resonance, electron cyclotron resonance, and

†Corresponding author. E-mail: e_yangx@126.com

© 2022 Chinese Physical Society and IOP Publishing Ltd 

upper hybrid resonance in homogeneous and inhomogeneous magnetized plasmas.[28] The studies mentioned above focused mainly on the transmission characteristics of electromagnetic waves in non-uniform magnetized plasma magnetized in a fixed direction and have obtained many meaningful conclusions. However, they considered neither the influence of magnetic field inhomogeneity nor the effect of the electric field on the plasma sheath. These external conditions will also affect the transmission of terahertz waves in the sheath to a certain extent.

In previous work, using the SMM, we compared and analyzed the transmission characteristics of the left and right-hand polarized THz waves when the various parameters changed.[29] However, we did not consider the non-uniform distribution of the magnetic field and did not add an electric field to the model to change the electron density distribution. Therefore, to explore the transmission characteristics of terahertz waves in the sheath more comprehensively, this paper considers the magnitude and direction of the inhomogeneous magnetic field, the influence of electric field on plasma density distribution and the collision frequency. Besides, the transmission performance before and after adding a magnetic field or electric field are compared. The SMM is also used in this work for calculation and analysis. Because the SMM makes fair use of the layering idea to reflect the inhomogeneity of plasma, by expressing the total electric and magnetic fields in each thin plasma layer, multiple reflections between layers can be considered. In addition, compared with the precise algorithm FDTD, it does not require a lot of meshes, and the transmittance can be calculated directly and efficiently. The SMM algorithm has low complexity and high computational efficiency, so it is very suitable for analyzing the plasma sheath. The rest of this article is arranged as follows. First, the total transmission model and the SMM model, and theoretical derivation are introduced. Then, before and after the electric or magnetic field is added, the transmission performance of the right-hand polarized terahertz wave in the plasma sheath is calculated and analyzed under different electron densities, magnetic field distributions, and different collision frequencies. Finally, some conclusions are drawn from the present studies.

## 2. Theory of SMM

We use the SMM to study the transmission characteristics of electromagnetic waves incident perpendicularly to the plasma sheath. The overall model used is shown in the cross-section of Fig. 1.

Electromagnetic waves enter into the plasma in a vertical direction. The magnet under the antenna provides a non-uniform magnetic field to magnetize the plasma sheath on the aircraft's surface. We simulate the magnetic field distribution of the magnet with the ANSYS Electronic Desktop V 19 and show the results from the model in Fig. 1. The simulation data will also be used in Section 3. In addition, in this model, we add positive electrode and negative electrode on the aircraft's surface to introduce an electric field. An electrostatic plasma sheath is formed when a negative voltage is applied to the negative electrode in a plasma. In the electrostatic plasma sheath, the electrons are depleted due to the applied negative voltage.[13] And electrodes and antenna can move synchronously according to the position we require. Because it is assumed that it is non-uniform only in the $x$-axis direction, we will analyze the transmission of THz waves in the plasma layer in the $xoy$ plane. Since magnetized plasma is a dispersive medium and possesses anisotropy, it can be divided into a certain number of thin layers with the same characteristics for analysis.

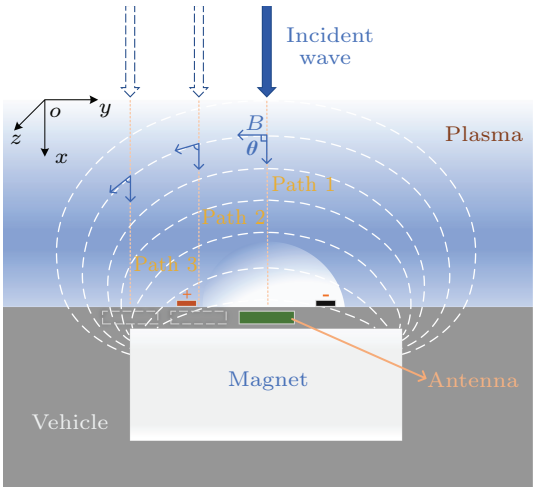



**Fig. 1.** Lumped model of terahertz wave incident on plasma under applied electromagnetic field.

As shown in the layered model in Fig. 2, the entire plasma sheath is divided into $n$ layers. The upper area (0) and lower area ($t$) are free spaces. Each layer of the layered plasma is regarded as a uniform plasma, and the propagation constant is $k^{(m)}$,

$$k^{(m)} = \frac{\omega}{c}\sqrt{\varepsilon_{\mathrm{r}}^{(m)}}, \tag{1}$$

where $\varepsilon_{\mathrm{r}}^{(m)}$ is the relative permittivity in the $m$-th layer of the sheet, $c$ is the speed of light in vacuum, and $\omega$ is the angular frequency of incident electromagnetic wave. The relative permittivity of the sheath is expressed by the Appleton formula[30]

$$\varepsilon_{\mathrm{r}}^{(m)} = 1 - \frac{Z}{X - \dfrac{Y\sin^2\theta}{2(X-Z)} \pm \left[\dfrac{Y^2\sin^4\theta}{4(X-Z)^2} + Y\cos^2\theta\right]^{1/2}}, \tag{2}$$

where sign $\pm$ represents the left polarization or right polarization; $\theta$ is the angle between the wave propagation path and the

magnetization direction; $X = 1 - \mathrm{i}\nu/\omega$, with $\nu$ being the collision angular frequency, and $\omega$ representing the incident electromagnetic wave angular frequency; $Y = \omega_{\mathrm{ce}}^2/\omega^2$, with $\omega_{\mathrm{ce}}$ being the electron cyclotron angular frequency; $Z = \omega_{\mathrm{p},m}^2/\omega^2$, with $\omega_{\mathrm{p},m}$ being the plasma angular frequency of the $m$-th layer.

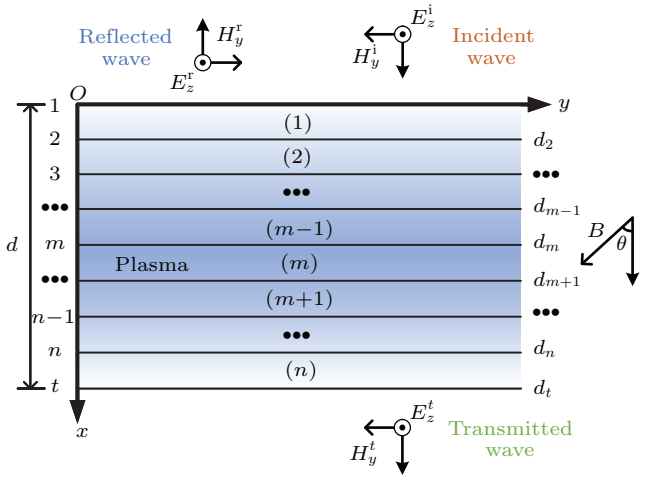



**Fig. 2.** Model of THz wave propagation in layered plasma.

The collision angular frequency can be expressed as[31]

$$\nu = 2 \times \pi \times 5.814 \times 10^{12} \frac{p}{p_0} \times T^{-1/2}, \tag{3}$$

where $p$ is the pressure, $T$ is the temperature, and $p$ is the standard atmospheric pressure.

The plasma angular frequency is expressed as[32]

$$\omega_{\mathrm{p},m} = \sqrt{\frac{N_{\mathrm{e}} e^2}{m_{\mathrm{e}} \varepsilon_0}}, \tag{4}$$

where $N_{\mathrm{e}}$ is the free electron density, $e$ and $m_{\mathrm{e}}$ are the electron charge and electron mass, respectively; $\varepsilon_0$ is the dielectric constant in a vacuum.

The electromagnetic field in the incident area 0 and the thin layer 1 in Fig. 1 are represented by the incident electric field $E_z^{\mathrm{i}}$, the reflected electric field $E_z^{\mathrm{r}}$, the incident magnetic field $H_y^{\mathrm{i}}$, and the reflected magnetic field $H_y^{\mathrm{r}}$. They are respectively written in the following forms:

$$\begin{cases} E_z^{\mathrm{i}(0)} = E_0 \mathrm{e}^{-\mathrm{i}k^{(0)}x}, \\ E_z^{\mathrm{r}(0)} = AE_0 \mathrm{e}^{\mathrm{i}k^{(0)}x}, \\ H_y^{\mathrm{i}(0)} = -\dfrac{E_0}{\eta_0} \mathrm{e}^{-\mathrm{i}k^{(0)}x}, \\ H_y^{\mathrm{r}(0)} = A\dfrac{E_0}{\eta_0} \mathrm{e}^{\mathrm{i}k^{(0)}x}, \end{cases} \tag{5}$$

$$\begin{cases} E_z^{\mathrm{i}(1)} = B_1 E_0 \mathrm{e}^{-\mathrm{i}k^{(1)}x}, \\ E_z^{\mathrm{r}(1)} = C_1 E_0 \mathrm{e}^{\mathrm{i}k^{(1)}x}, \\ H_y^{\mathrm{i}(1)} = -B_1\dfrac{E_0}{\eta_1} \mathrm{e}^{-\mathrm{i}k^{(1)}x}, \\ H_y^{\mathrm{r}(1)} = C_1\dfrac{E_0}{\eta_1} \mathrm{e}^{\mathrm{i}k^{(1)}x}, \end{cases} \tag{6}$$

where $A$ is the reflection coefficient incident on the surface of the first plasma layer; $B_1$ is the transmission coefficient of the electromagnetic wave from the area 0 into the plasma layer 1; $C_1$ is the reflection coefficient of the electromagnetic wave from plasma layer 2 back to plasma layer; $k^{(0)}$ is the wave number in free space. In this way, the total electromagnetic field relationship between the incident area 0 and the thin layer 1 can be determined, and the matrix relation can be obtained by the imposed boundary conditions of the interface at $x = 0$:

$$\begin{pmatrix} B_1 \\ C_1 \end{pmatrix} = S_1 \begin{pmatrix} A \\ 1 \end{pmatrix}, \tag{7}$$

where

$$S_1 = \frac{1}{2k_x^{(1)}} \begin{pmatrix} k_x^{(1)} - k_x^{(0)} & k_x^{(1)} + k_x^{(0)} \\ k_x^{(1)} + k_x^{(0)} & k_x^{(1)} - k_x^{(0)} \end{pmatrix}. \tag{8}$$

In the same way as the above, continuing to match the next interface until the $n$-th yields the matrix equation as follows:

$$\begin{pmatrix} B_m \\ C_m \end{pmatrix} = S_m \begin{pmatrix} B_{m-1} \\ C_{m-1} \end{pmatrix}, \tag{9}$$

where

$$S_m = \begin{pmatrix} \mathrm{e}^{-\mathrm{i}k_x^{(m)}d_m} & \mathrm{e}^{\mathrm{i}k_x^{(m)}d_m} \\ k_x^{(m)}\mathrm{e}^{-\mathrm{i}k_x^{(m)}d_m} & -k_x^{(1)}\mathrm{e}^{\mathrm{i}k_x^{(m)}d_m} \end{pmatrix}^{-1} \times \begin{pmatrix} \mathrm{e}^{-\mathrm{i}k_x^{(m-1)}d_m} & \mathrm{e}^{\mathrm{i}k_x^{(m-1)}d_m} \\ k_x^{(m-1)}\mathrm{e}^{-\mathrm{i}k_x^{(m-1)}d_m} & -k_x^{(m-1)}\mathrm{e}^{\mathrm{i}k_x^{(m-1)}d_m} \end{pmatrix}. \tag{10}$$

The left and right of the last interface are the plasma layer ($n$) and free space ($t$). There are only transmitted electromagnetic waves in the area ($t$) but no reflected electromagnetic waves. Therefore, matching the boundary conditions at $x = d$ can obtain a matrix equation

$$\begin{pmatrix} B_n \\ C_n \end{pmatrix} = V_t \cdot D, \tag{11}$$

where $D$ is the total transmission coefficient and

$$V_t = \frac{1}{2k_x^{(n)}} \begin{pmatrix} (k_x^{(n)} + k_x^{(t)})\mathrm{e}^{\mathrm{i}(k_x^{(n)} - k_x^{(t)})d_t} \\ (k_x^{(n)} - k_x^{(t)})\mathrm{e}^{-\mathrm{i}(k_x^{(n)} + k_x^{(t)})d_t} \end{pmatrix}. \tag{12}$$

Through the above formulas (7), (9), and (11), we can recursively transform and obtain

$$S_{\mathrm{g}} \begin{pmatrix} A \\ 1 \end{pmatrix} = V_t \cdot D, \tag{13}$$

where

$$S_{\mathrm{g}} = S_n \cdot S_{n-1} \cdot S_{n-2} \cdots S_1 = \left( \prod_{m=n}^{2} S_m \right) S_1. \tag{14}$$

Next, $S_g = (S_{g1}, S_{g2})$, where $S_{g1}$ and $S_{g2}$ represent the first vector and the second column vector of $S_g$, so formula (13) can be transformed into

$$\begin{pmatrix} S_{g1} & -V_t \end{pmatrix} \begin{pmatrix} A \\ D \end{pmatrix} = -S_{g2}. \tag{15}$$

Finally, the matrix of coefficients $A$ and $D$ can be written as follows:

$$\begin{pmatrix} A \\ D \end{pmatrix} = -\begin{pmatrix} S_{g1} & -V_t \end{pmatrix}^{-1} \cdot S_{g2}. \tag{16}$$

Then the normalized transmission power of electromagnetic wave is expressed as $|D|^2$.

## 3. Numerical results and discussion

This part will discuss the transmission characteristics of the right-hand polarized terahertz wave in the plasma sheath under different parameters after having added a magnetic field and an electric field. According to the plasma parameter electrostatic probe measurement data of NASA's reentry flight test,[1] the double Gaussian distribution can approximate the electron density distribution of the aircraft surface sheath and the specific distribution model expression is given below:

$$N_e = \begin{cases} N_0 \exp\left(-a(x-x_0)^2\right), & (0 \le x < x_0), \\ N_0 \exp\left(-b(x-x_0)^2\right), & (x_0 \le x < d). \end{cases} \tag{17}$$

Note that $N_0$ in this model indicates the maximum of the plasma electron density, and $d$ is the thickness of the plasma layer. The coefficient is set to be $a = 300$, $b = 220$, $d = 0.1$, and $x_0 = 0.06$, respectively, to determine the position of the maximum electron density in the incident path. The specific distribution is shown in Fig. 3(a).

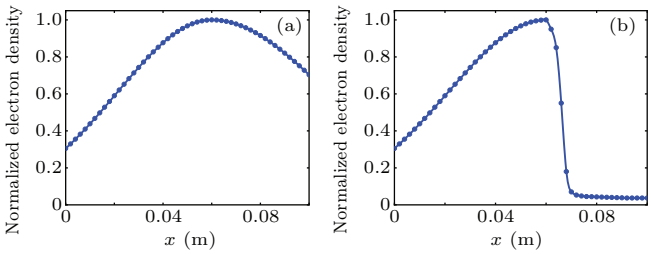



**Fig. 3.** Electron density distribution of (a) before and (b) after adding electric field.

Research shows that an electrostatic plasma sheath is formed when a negative voltage is applied to a negative electrode in a plasma. In the electrostatic plasma sheath, the electrons are depleted due to the applied negative voltage, forming a low electron density area.[3,6,13] These researches show that when a $-1000$ V potential drop is applied across the two electrodes in plasma with an electron density of $1 \times 10^{18}$ m$^{-3}$, a low electron density area will be generated around the negative electrode with a radius of about 3 cm to 4 cm. Thus in our work, we assume that the voltage applied to the positive electrode and negative electrode are 0 V and $-1000$ V, respectively, and assume that the radius of the low electron density region formed by the electric field is about 3 cm. Here we do not consider the distribution of electric fields for the time being. Figure 3(b) shows the radial electron density distribution when an electric field is added.

To verify the accuracy of the SMM in our work, we find other two research results and compare them. From Ref. [33], we can obtain an experimental result. From Ref. [18], we can obtain a simulated result based on the FDTD method under the same parameters. The absorption coefficient obtained separately by the SMM method, by the FDTD method and in experiment are demonstrated in Fig. 4. Here, $d = 0.15$ m, $N_0 = 7.9 \times 10^{18}$ m$^{-3}$, and $\nu = 1.6 \times 10^{11}$ s$^{-1}$. We can observe that the simulated results by SMM are in good agreement with the results by accurate algorithm FDTD, and the locations of the absorption peaks in the two simulated results are very close to the experimental data. The difference between the simulation and the experimental data is considered to be caused by external conditions and by the parameter settings of the plasma.

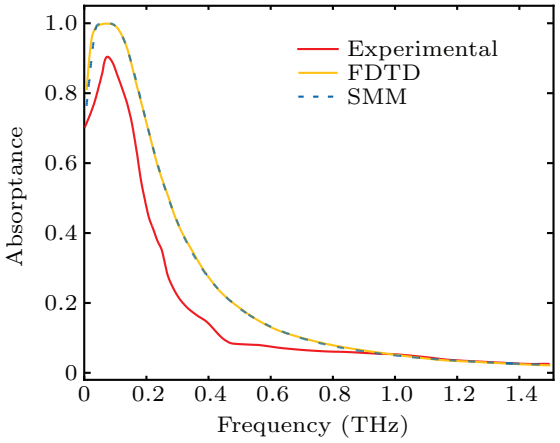



**Fig. 4.** Plots of absorption coefficient of two simulation results and experimental results.

On this basis, the SMM can be used to calculate the influence of the external magnetic field and the external electric field on the transmission characteristics of terahertz wave in the plasma sheath. The peak electron density is an essential factor affecting the transmission of terahertz wave. Figure 5 shows the variations of normalized transmission power with frequency when the maximum electron density $N_0$ is $1 \times 10^{17}$ m$^{-3}$, $1 \times 10^{18}$ m$^{-3}$, and $1 \times 10^{19}$ m$^{-3}$. At this time, the total thickness of plasma plate is $d = 10$ cm, the number of layers is $n = 50$, the collision frequency is $f_\nu = 50$ GHz, and the magnetic field strength is $B = 0$ T or $B = 3$ T. As the maximum electron density increases, the transmission power decreases, gradually forming a completely non-transmissible stop band at the low-frequency end. Figure 5(a) shows the

comparison among the effects of adding a magnetic field to the transmission power for three different maximum electron densities. When electromagnetic waves propagate in a plasma with an external magnetic field, the electrons in the plasma will be subjected to a magnetic field to make a cyclotron motion. The right-hand polarized wave will rotate synchronously with the cyclotron electrons to form a cyclotron resonance, resulting in energy absorption. We can see that when $N_0 = 1 \times 10^{17}$ m$^{-3}$, $B = 3$ T, and the magnetic field perpendicular to the incident direction of the terahertz wave, due to cyclotron resonance, the transmission power will first decrease and then increase with the increase of the wave frequency, forming a protruding peak, and the frequency corresponding to the top of the peak is near the cyclotron frequency. Comparing with the situation of no magnetic field, the transmission power increases at the low-frequency end, which is more conducive to the passage of electromagnetic waves. However, without a magnetic field, the THz wave shows better transmission in the high-frequency band. When the electron density increases to a certain value, a transmission stopband appears, and a magnetic field will make the stopband wider, but not conducive to electromagnetic wave transmission. Figure 5(b) shows the comparison among the electric field's influences on the transmission power when there is no magnetic field. It can be seen that the transmission power increases to a certain extent after the electric field is added, and it is more evident at high electron density. In addition, we also investigate the case of adding the magnetic field and electric field at the same time. The influence on the transmission under the combined action of the magnetic field and the electric field is just the superposition of Fig. 5(a) and Fig. 5(b), so we will not analyze it here.

According to the model in Fig. 1, since the magnitude and direction distribution of the magnetic induction intensity provided by the permanent magnet is not uniform, the angle $\theta$ between the incident electromagnetic wave and the magnetic field intensity vector will change due to different wave propagation positions. Figure 6 shows the magnetic field intensity distributions and direction distributions along the three paths above the permanent magnet simulated by the ANSYS Electronic Desktop V 19. Here we assume that the permanent magnet can achieve a sufficient large magnetic field intensity.

Figure 7 shows the variations of transmission power of terahertz wave with frequency when the wave is normally incident on the sheath along the three paths in Fig. 1. We can see that the magnetic field magnitude distribution along path 1 is not much different from along path 2. Still, the transmission performance along path 1 is better than along path 2. We can infer that the distribution of the magnetic field direction affects the transmission performance. Therefore, we will analyze the magnitude and direction of the magnetic field below separately.

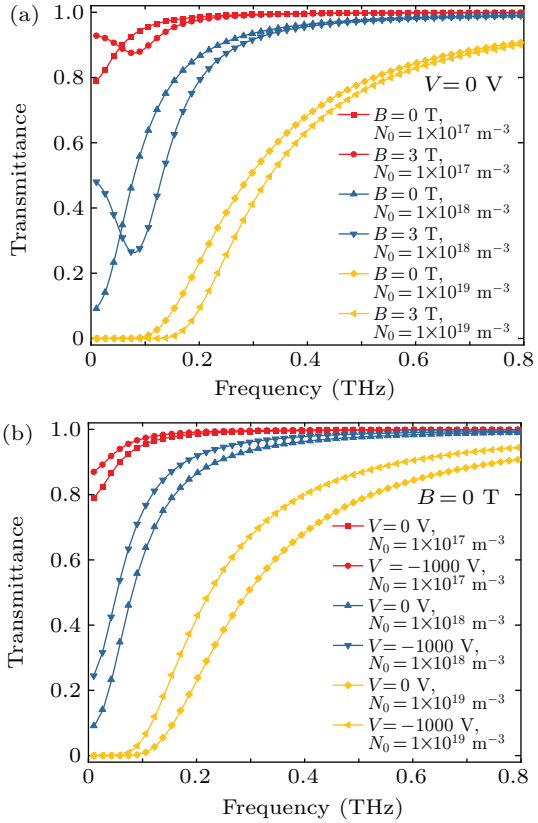



**Fig. 5.** Influences of separately applied magnetic field and electric field on transmission under different electron densities (a) without electric field and (b) without magnetic field.

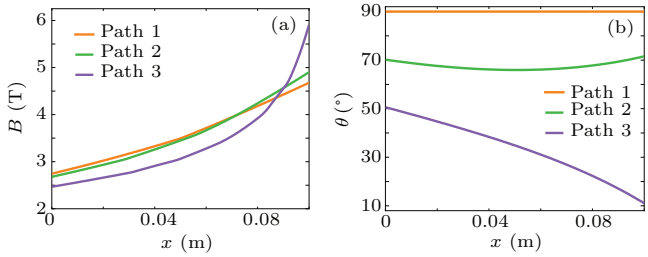



**Fig. 6.** Distributions of (a) magnitudes and (b) directions of magnetic field along three paths.

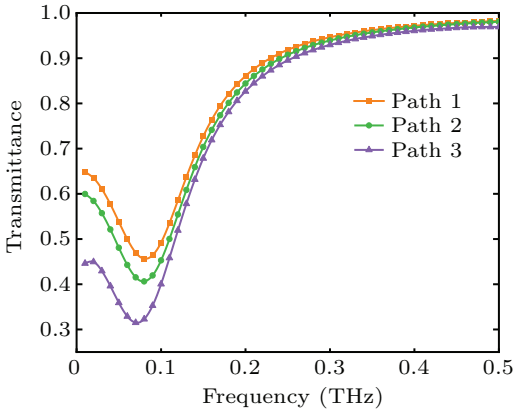



**Fig. 7.** Variations of normalized transmission power with frequency along three paths.

As shown in Fig. 8, the maximum electron density is $N_0 = 1 \times 10^{18}$ m$^{-3}$, the collision frequency is $f_v = 50$ GHz, and the potential applied to the negative electrode is $V = -1000$ V. The magnetic field strengths in Fig. 8(a) are 1 T, 3 T, 5 T, respectively, and the magnetization angle is 90°. In the meantime, figure 8(b) shows the transmission coefficients when the magnetic field intensity is set to be 3 T, and the magnetization angles are 30°, 60°, and 90°, respectively. Figure 8(a) shows that with the magnetic field strength increasing, the absorption peaks move toward higher frequencies due to the cyclotron resonance effect. However, the absorption bandwidth is almost unchanged, so the transmission power at the low-frequency end is much improved, and the transmission performance at the high-frequency end is weakened. On the other hand, as shown in Fig. 8(b), as the angle between the direction of the magnetic field and the propagation path increases, the transmission power increases to a certain extent. In this way, by controlling the strength and direction of magnetic field, electromagnetic wave at a specific frequency can better pass through the plasma sheath.

Figure 9 shows the variations of the normalized transmission power with frequency of terahertz waves in the plasma sheath under different collision frequencies. Figures 9(a)–9(c) correspond to different situations: none of magnetic field and electric field, only magnetic field, both magnetic and electric fields. At this time, the values of the collision frequency $f_v$ are 10 GHz, 50 GHz, 100 GHz, and 200 GHz, respectively, the maximum electron density is $N_0 = 1 \times 10^{18}$ m$^{-3}$, the potential is $V = 0$ V or $V = -1000$ V, and the magnetic field strength is 0 T or 3 T. We can see that the increase of collision frequency can also increase the transmission power at the low-frequency end, and the high collision frequency can inhibit the energy absorption caused by cyclotron resonance to some extent when a magnetic field is added. This result is due to frequent collisions between electrons, ions, and neutral particles, which weakens the cyclotron motion of electrons in the magnetic field. In this case, the absorption peak decreases, which is more conducive to transmitting right-polarized terahertz waves in a particular frequency band. Besides, after the electric field is added, the transmission power trend in the frequency band is almost unchanged, but the value is improved to a certain extent, which is more conducive to the transmission.

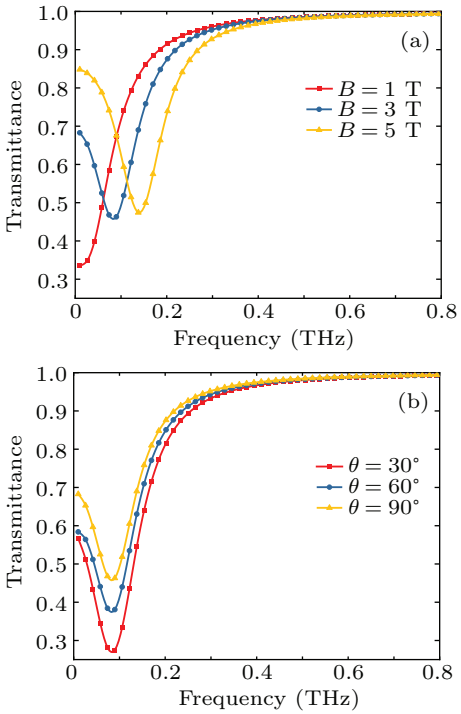



**Fig. 8.** Variations of of transmission power with frequency of THz wave (a) at different strengths and (b) in different directions of magnetic field strengths.

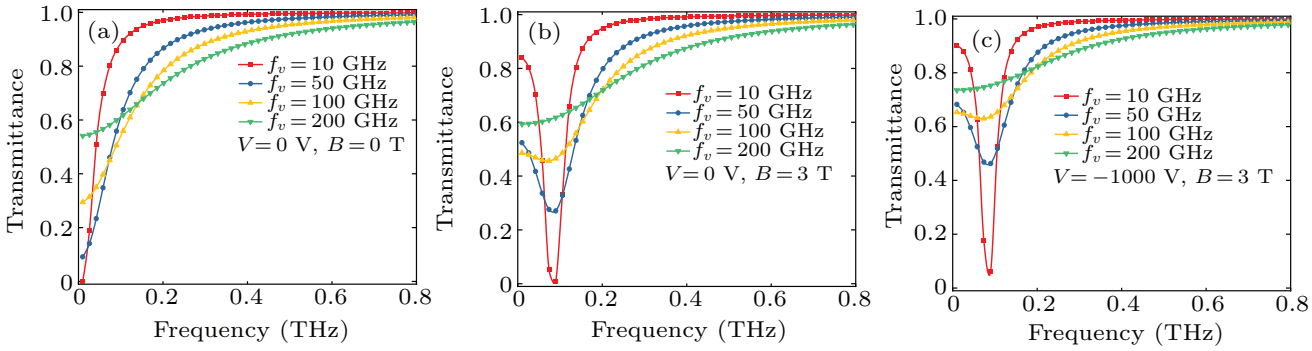



**Fig. 9.** Influences of the collision frequency on the THz wave transmission at (a) $V = 0$ V and $B = 0$ T, (b) $V = 0$ V and $B = 3$ T, (c) $V = 1000$ V and $B = 3$ T.

## 4. Conclusions

In this work, both a magnetic field and an electric field are used to improve the transmission performance of terahertz wave in the sheath, considering the inhomogeneity of the magnetic field strength and direction distribution to the antenna window. The SMM is adopted to calculate and analyze the influences of maximum electron density, magnetic field magnitude, magnetic field direction, and collision frequency on the transmission power of right-hand polarized terahertz waves after adding a magnetic field or electric field. The calculation results show that the maximum electron density significantly affects the transmission of terahertz wave. The higher

the electron density, the less the electromagnetic wave energy remains after passing through the sheath. After adding a magnetic field to the antenna window, the electromagnetic wave transmission power at the low-frequency end can increase to a certain extent, but it is not conducive to electromagnetic wave transmission with a frequency is near the cyclotron frequency. Both the strength and direction of magnetic field can improve the transmission performance of electromagnetic waves in the sheath to a certain extent. The magnetic field's distribution perpendicular to the transmission direction is most conducive to transmitting right-hand polarized terahertz waves. Increasing the collision frequency can alleviate the energy absorption caused by cyclotron resonance to a certain extent. By appropriately adjusting the above parameters, the ability of electromagnetic waves to transmit in the plasma sheath at a particular frequency can be improved to a certain extent, and the blackout problem can be improved.

## Acknowledgements

Project supported by the Open Foundation of Semiconductor Power Device Reliability Engineering Research Center of Ministry of Education, China (Grant No. ERCMEKFJJ2019-(05)), the Natural Science Foundation of Guizhou University, China (Grant No. (2019)62), and the China Scholarship Council (Grant No. 202106675002).

## References

[1] Dunn M G and Kang S W 1973 *Theoretical and Experimental Studies of Reentry Plasmas* (Washington: National Aeronautics and Space Administration) NASA-CR-2232
[2] Gupta R N, Yos J M, Thompson R A and Lee K P 1990 *A Review of Reaction Rates and Thermodynamic and Transport Properties for an 11-species Air Model for Chemical and Thermal Nonequilibrium Calculations to* 30000 K (Hampton: Langley Research Center) NASA-RP-1232
[3] Keidar M, Kim M and Boyd I D 2008 *J. Spacecr. Rockets* **45** 445
[4] Rybak J P and Churchill R J 1971 *IEEE Trans. Aerosp. Electron. Syst.* **7** 879
[5] Cook D J and Hochstrasser R M 2000 *Opt. Lett.* **25** 1210
[6] Kim M, Keidar M and Boyd I D 2008 *J. Spacecr. Rockets* **45** 1223
[7] Gillman E D, Foster J E and Blankson I M 2010 *Review of Leading Approaches for Mitigating Hypersonic Vehicle Communications Blackout and a Method of Ceramic Particulate Injection Via Cathode Spot Arcs for Blackout Mitigation* (Washington: National Aeronautics and Space Administration) NASA-TM-2010-216220
[8] Shi L, Guo B L, Liu Y M and Li J T 2012 *Prog. Electromagn. Res.* **123** 321
[9] Gao X and Jiang B 2015 *J. Appl. Phys.* **117** 233301
[10] Zhou H, Li X, Liu Y, Bai B and Xie K 2017 *IEEE Trans. Plasma Sci.* **45** 15
[11] Zhang Y Y, Xu G J and Zheng Z Q 2019 *Optik* **182** 618
[12] Lemmer K M, Gallimore A D, Smith T B, Davis C N and Peterson P 2009 *J. Spacecr. Rockets* **46** 1100
[13] Kim M, Keidar M and Boyd I D 2008 *IEEE Trans. Plasma Sci.* **36** 1198
[14] Kalluri D K, Goteti V R and Sessler A M 1993 *IEEE Trans. Plasma Sci.* **21** 70
[15] Hu B J, Wei G and Lai S L 1999 *IEEE Trans. Plasma Sci.* **27** 1131
[16] Lv C J, Cui Z W and Han Y P 2019 *Chin. Phys. B* **28** 74203
[17] Chu Q X and Ding H 2006 *IEEE Trans. Magn.* **42** 3141
[18] Yuan C X, Zhou Z X, Zhang J W, Xiang X L, Yue F and Sun H G 2011 *IEEE Trans. Plasma Sci.* **39** 1577
[19] Tian Y, Han Y P, Ling Y J and Ai X 2014 *Phys. Plasmas* **21** 23301
[20] Liu S, Chen S, He Z F, Zhong S Y and Wang H Q 2015 *Wave. Random Complex* **25** 393
[21] Tian Y X, Yan W Z, Gu X L, Jin X L, Li J Q and Li B 2017 *AIP Adv.* **7** 125325
[22] Cong C, Shi C and Shi Z 2018 *Optik* **159** 69
[23] Rahmani Z, Moradi H and Tazimi N 2020 *Indian J. Phys.* **94** 935
[24] Rao Q W, Xu G J, Wang P F and Zheng Z Q 2021 *Sensors* **21** 263
[25] Chen A T, Sun H Y, Han Y P, Wang J J and Cui Z W 2019 *Chin. Phys. B* **28** 14201
[26] Yu H, Xu G J and Zheng Z Q 2019 *Optik* **188** 244
[27] Guo L J, Guo L X, Li J T and Ai X 2017 *Phys. Plasmas* **24** 22108
[28] Zhang J, Fu H Y and Scales W 2018 *IEEE Trans. Plasma Sci.* **46** 2146
[29] Li H, Yang X and Zhang Z P 2021 *Acta Phys. Sin.* **70** 075202 (in Chinese)
[30] Heald M A, Wharton C B and Furth H P 1965 *Phys. Today* **18** 72
[31] Ouyang W C, Jin T, Wu Z W and Deng W F 2021 *IEEE Trans. Plasma Sci.* **49** 460
[32] Yeh C and Rusch W V T 1965 *J. Appl. Phys.* **36** 2302
[33] Yuan C X, Zhou Z X, Xiang X L, Sun H G and Pu S Z 2010 *Phys. Plasmas* **17** 113304